Ultra-fast analysis of peptides by laser diode thermal desorption-triple quadrupole mass spectrometry

Pedro A. Segura [1,*], Cédric Guillaumain [1], Emmanuel Eysseric [1], Judith Boudrias [1], Mégane Moreau [1], Cassandra Guérette [1], Rémi Clémencin [1], Francis Beaudry [2,3]

* Tel: 1-(819) 821-7922. E-mail: pa.segura@usherbrooke.ca

[1] Department of Chemistry, Faculty of Sciences, Université de Sherbrooke, Sherbrooke, QC, Canada

[2] Département de Biomédecine Vétérinaire, Faculté de Médecine Vétérinaire, Université de Montréal, Saint-Hyacinthe, QC, Canada

[3] Centre de recherche sur le cerveau et l'apprentissage (CIRCA), Université de Montréal, Montréal, Québec, Canada

Abstract

Rationale: The COVID-19 pandemic demonstrated the importance of high-throughput analysis for public health. Given the importance of surface viral proteins for interactions with healthy tissue, they are targets of interest for mass spectrometry-based analysis. For that reason, the possibility of detecting and quantifying peptides using a high-throughput technique, laser diode thermal desorption-triple quadrupole mass spectrometry (LDTD-QqQMS), was explored.

Methods: Two peptides used as models for small peptides (leu-enkephalin and endomorphin-2) and four tryptic peptides (GVYYPDK, NIDGYFK, IADYNYK, and QIAPGQTGK) specific to the SARS-CoV-2 Spike protein were employed. Target peptides were analyzed individually in the positive mode by LDTD-QqQMS. Peptides were quantified by internal calibration using multiple reaction monitoring transitions in pure solvents and in samples spiked with 20 μg mL^{-1} of a bovine serum albumin tryptic digest to represent real analysis conditions.

Results: Low energy fragment ions (*b*- and *y*- ions) as well as high-energy fragment ions (*c*- and *x*-ions) and some of their corresponding water or ammonia losses were detected in the full mass spectra. Only for the smallest peptides, leu-enkephalin and endomorphin-2, $[M+H]^+$ ions were observed. Product ion spectra confirmed that, with the experimental conditions used in the present study, LDTD transfers a considerable amount of energy to the target peptides. Quantitative analysis showed that it was possible to quantify peptides using LDTD-QqQMS with acceptable calibration curve linearity (R^2>0.99), precision (RSD<18.2%), and trueness (bias<8.3%).

Conclusions: This study demonstrated for the first time that linear peptides can be qualitatively and quantitatively analyzed by LDTD-QqQMS. Limits of quantification and dynamic ranges are still inadequate for clinical applications, but other applications where higher levels of proteins must be detected, could be possible by LDTD. Given the high-throughput capabilities of LDTD-QqQMS (> 15000 in less than 43 h), more studies are needed to improve the sensitivity for peptide analysis of this technique.

Keywords: severe acute respiratory syndrome coronavirus 2 (SARS-CoV-2), endomorphin-2, leucine enkephalin, atmospheric pressure chemical ionization, high-throughput, peptide quantification.

1. Introduction

In December 2019, an outbreak of a novel coronavirus (SARS-CoV-2) infection emerged and has rapidly spread worldwide representing a significant threat to humans [1]. The coronavirus disease (COVID-19) is the result of a SARS-CoV-2 viral infection. Over two years after the initial outbreak, the COVID-19 pandemic continues worldwide, and rapid diagnostic tools to fight the virus's spread are at the centre of public health organization's strategy [2-4]. The SARS-CoV-2 virus particles include the RNA genetic material and structural proteins required for cell invasion. The Spike protein is found on the outside of the virus particle and mediates attachment of the virus particle and entry into the cell. Specifically, the Spike protein interacts with the angiotensin-converting enzyme 2, an enzyme that can be found attached to the membrane of cells [5, 6]. Consequently, the Spike protein is an important target for vaccine development, antibody therapies and diagnostic tests [7-9]. Very rapidly, reverse transcription polymerase chain reaction methods for SARS-CoV-2 detection were developed, validated, and used to test millions of people but it put a strain on the health care systems of many countries around the globe [10, 11]. The demand for rapid and cost-effective analysis methods is important to fight the spread [12]. Antigen rapid diagnostic tests for SARS-CoV-2 are now very commonly used, but they have several limitations including lack of sensitivity and specificity and they are effective for the detection of the original Wuhan strain, but they are much less effective to detect new variants [13]. The COVID-19 pandemic has demonstrated the importance of high-throughput analysis techniques in public health.

There is no doubt that, mass spectrometry (MS) occupies a central role in modern bioanalysis and as such multiple high-throughput mass spectrometry techniques have been developed in the past ten years [4-6]. Furthermore, MS has become a workhorse in proteomics [14-16]. Multiple reaction monitoring (MRM) mass spectrometry has been widely successfully applied to detect and quantify targeted proteins in biological samples using bottom-up approaches [17-19]. Bottom-up proteomics involves proteolytic digestion, typically trypsin digestion of proteins prior analysis by MS [20]. MRM-MS is a targeted technique distinctive from the analytical strategies used in discovery proteomics (i.e., shotgun proteomics). MRM-based methods are at the centre of rapid developments in protein and biomedical research. Typically, MRM is performed on triple quadrupole mass spectrometers (QqQ) allowing to target specific tryptic peptides of interest and provides superior specificity and sensitivity [19]. The first quadrupole mass analyzer is used to isolate the precursor (peptide) ion, then fragmented in the collision cell to generate product ions and finally, a small number of sequence-specific fragment ions, typically 2 or 3, are isolated in the second quadrupole mass analyzer. The precursor/product ion transitions are selected to enhance specificity and sensitivity. Moreover, the use of spiked-in, stable isotope-labelled peptides permit precise quantification [21, 22]. *In silico* full mass and tandem mass libraries can be generated and maintained based on SARS-CoV-2 surveillance and sequencing performed by public health agencies assisting MRM-MS quantification of specific tryptic peptides of viral proteins from the original and variant strains. However, the application of MRM-based assays for large-scale analysis is limited. Liquid chromatography (LC) or derivative techniques are commonly hyphenated to QqQ MS for targeted MRM-based proteomic assays. The LC run-time is an important limitation significantly diminishing the throughput but also increasing the analysis cost. However, a question remains; can we use MRM-based assays to detect specific tryptic peptides associated to viral proteins, more specifically, the Spike protein found on the viral particle of the

SARS-CoV-2? Such assays require high-throughput techniques to cope with the high number of tests required by public health agencies.

Laser diode thermal desorption (LDTD) is a mature sample desorption and ion source for mass spectrometry designed for high-throughput analysis that has been applied successfully to a large array of small molecules such as hormones [23], antibiotics [24-27], pharmaceuticals [28-31], and pesticides [32, 33] in complex biological or environmental matrices. In LDTD, samples are thermally desorbed rapidly by an infrared laser that hits the back of the microwell plate where samples are deposited. Thus, contrary to MALDI, there is no contact between the laser and the sample. Desorbed molecules in the gas phase are then transported by a carrier gas towards a corona needle where molecules in the gas phase are ionized by atmospheric pressure chemical ionization (APCI). The carrier gas, typically air containing traces of water, also induces thermalization of the desorbed molecules thus reducing thermal degradation and allowing proper ionization [24]. Despite this thermal desorption process, extensive molecular fragmentation in LDTD has not been reported and to the authors' knowledge only loss of water has been observed in the analysis of hormones [23]. However, the application of LDTD to the quantitative analysis of peptides remains unexplored. It has been demonstrated that APCI can be employed to ionize large peptides, e.g., angiotensin I (1296 Da) [34], and even proteins [35] with minimal fragmentation. Therefore, the major challenge for the quantitative analysis of peptides by LDTD is low thermal desorption efficiency and the sensitivity of peptides to high temperatures.

The effect of high temperatures on peptide ions has been extensively studied by MS in the last 30 years [36-41]. In an early report on thermal decomposition of peptides, Meot-Ner, et al. [36] ionized leu-enkephalin by electrospray ionization (ESI) and then passed it through a wide-bore reactor tube heated at 385 °C or 406 °C. They observed that fragment ions such as a_4, b_4+18, and $[M+H-18]^+$ were among the most abundant ions in the mass spectrum. According to the authors of that report, thermal decomposition is not expected to generate *b*-ions but rather *a*-ions since it is a rather low energy process. Later, Chen, et al. [37] used a similar setup, based on electrosonic spray ionization and a coiled tube heated between 230 and 380 °C, to investigate the thermal dissociation of peptides angiotensin II and bradykinin. They observed a_n, b_n, and y_n-ions as well as fragment ions resulting from loss of H_2O or NH_3. Meetani, et al. [39] used pyrolysis between 200 and 220°C and observed the formation of cyclic oligopeptides, cyclic oligopeptides with losses of side groups, and fragmentation of the peptide backbone to yield b_n, y_n, c_n, z_n, and a_n, x_n-ions as well as v_n and w_n-ions. Basile, et al. [40] and Zhang and Basile [38] also induced the thermal cleavage of a series of peptides using a pyrolizer device at 220 °C and ionized the degradation products by electrospray. They observed $[M+H|^+$, $[M-H_2O+H]^+$, $[M-NH_3+H]^+$ or $[M-2NH_3+H]^+$ ions as well as specific cleavages at the C-terminal side of aspartic acid or the N-terminus of cysteine. Finally, Altmeyer, et al. [41] investigated the thermal fragmentation of peptides by using superheated water at several temperatures between 120 and 200 °C. In that study, the authors observed superheating-induced fragmentation that yielded mainly *y*-ions.

LDTD-QqQMS method could reduce analysis time by several orders of magnitude (i.e. ≈10 s per sample), compared to more conventional LC-QqQMS approaches. Therefore, the objective of the present study is first to identify the ions generated by LDTD for six target peptides and then evaluate if MRM transitions could be employed for quantitative analysis of peptides in samples spiked with a protein digest.

2. Methods

2.1 Chemicals and reagents

Standards of endomorphin-2 (YPFF-NH_2, ≥97 %) and leu-enkephalin (YGGFL) acetate salt hydrate (≥ 95 %), were purchased from Phoenix Pharmaceuticals (Burlingame, CA) and Sigma-Aldrich Canada (Oakville, ON), respectively. Four tryptic peptides specific to the SARS-CoV-2 Spike protein from the Wuhan strain were chosen according to an *in silico* analysis made by Orsburn, et al. [42]. The peptide sequences were: GVYYPDK, NIDGYFK, IADYNYK, and QIAPGQTGK. These tryptic peptides were custom-synthetized by CanPeptide (St-Laurent, QC) and had a purity of 95 % or better. Isotopically labelled leu-enkephalin [YGGF(d_5)L], endomorphin-2 [YPFF(d_5)-NH_2], G(d_2)VYYPDK, IAD(d_4)YNYK, and QIA(d_4)PGQTGK were also custom-synthetized by CanPeptide (St-Laurent, QC) and had purity of 95 % or better. Bovine serum albumin (BSA) and trypsin from porcine pancreas were purchased from Sigma-Aldrich Canada. Methanol (MeOH) and water (LC-MS grade) as well as potassium phosphate dibasic (K_2HPO_4) were purchased from Fisher Scientific (Ottawa, ON). Stock solutions of the four tryptic peptides specific to the SARS-CoV-2 Spike protein were prepared in LC-MS grade water at a concentration of 1000 μg mL^{-1} and were kept at 4 °C. Stock solutions of endomorphin-2 and leu-enkephalin were prepared in LC-MS grade water at a concentration of 100 μg mL^{-1} and 700 μg mL^{-1} respectively and were kept at 4 °C.

2.2 Sample preparation

LazWell microwell plates, made of stainless-steel 316L, and manufactured by Phytronix (Québec, QC) were used in all experiments. For the detection and identification of ions using the full scan mode, peptide solutions were prepared in MeOH-H_2O (3:1, *v/v*) to obtain a peptide concentration of between 25 and 50 μg mL^{-1}. Aliquots of 4 μL were then deposited on the LazWell microwell and dried for 5 min.

For the quantification of the peptides in the solvent using the MRM mode, peptide solutions were prepared in MeOH-H_2O (3:1, *v/v*) and mixed with 15 mM of phosphate buffer adjusted to pH 8 and 10 μg mL^{-1} of the deuterated analogue. Experiments showed that addition of the phosphate buffer was necessary to improve signals for most of the peptides (Figure S1). Different peptide concentrations were prepared between 1 μg mL^{-1} to 40 μg mL^{-1} depending on the peptide. Aliquots

of 4 µL were then deposited on the LazWell microwell and dried for 5 min. 4 replicates were performed.

For the quantification of the peptides spiked in digested BSA using the MRM mode, peptide solutions were prepared in MeOH-H_2O (3:1, *v/v*) and mixed with 15 mM of phosphate buffer adjusted to pH 8, 20 µg mL^{-1} of digested BSA and 10 µg mL^{-1} of the deuterated analogue. Different peptide concentrations were prepared between 0.01 µg mL^{-1} to 40 µg mL^{-1} depending on the peptide. Aliquots of 4 µL were then deposited on the LazWell microwell and dried for 5 min. Four replicates were performed per analyte.

2.3 Analysis by LDTD-QqQMS

Thermal desorption and ionization of samples were performed using an LDTD source model W-960 from Phytronix. Mass analysis and detection were done by a Xevo TSQ-micro triple-quadrupole mass spectrometer from Waters (Milford, MA, USA) on which the LDTD source was mounted. Laser power pattern was as follows: increase from 0 to 100% in 6 s, stay at 100% for 4 s, and return to 0% immediately. Flow rate of compressed air used as carrier gas was set to 3 L min^{-1}. Peptides were ionized by atmospheric pressure chemical ionization (APCI) in the positive mode.

2.4 Predicted peptide fragment ions

MS-Product, a peptide mass spectrometry utility from ProteinProspector version 6.3.1, developed by the University of California, San Francisco (https://prospector.ucsf.edu/prospector/cgi-bin/msform.cgi?form=msproduct) was employed to simulate the fragmentation of target peptides and identify the ions observed.

2.5. Quantitative analysis

Acquisition was carried out in the MRM mode and the transitions used are shown on Table S1 (Supporting Information). Data were processed using MassLynx Software version 4.2 from Waters. Quantification was done by internal calibration using deuterated analogues of the peptides. Internal calibration curves were determined using ordinary least squares linear regression based on the average of four replicate measurements per concentration level. Limits of detection (LOD) were determined according to the IUPAC definition employing a value of k=3 [43]. Limits of quantification (LOQ) were defined as concentration of the lowest standard with a bias percentage ≤ ±20 %. The dynamic range was defined by the concentration interval between the LOQ and the highest point of the calibration curve.

3. Results and discussion

3.2 Full scan spectra of peptides ionized by LDTD

Total ion current desorption profiles and full mass spectra of the target peptides are shown in Figures S1 to S6 (Supporting information). Desorption profiles were for the most part atypical of LDTD [23, 27, 44]. Peaks were generally asymmetric with a tailing, and peak splitting was also observed for endomorphin-2. In LDTD, tailing peak shapes are indicative of a slow thermal desorption [45]. Peak splitting suggests signal suppression due to a high number of species desorbed simultaneously [45].

Results showed that peaks corresponding to the $[M+H]^+$ ion with both high abundance and high signal-to-noise ratio were only observed for the two smaller peptides, leu-enkephalin and endomorphin-2. $[M+2H]^{2+}$ ions were only observed for IADYNYK (*m/z* 886) and QIAPGQTGK (*m/z* 899) and only in the case of the latter, its relative abundance was high (20.4%). These results thus suggest that the laser power pattern used to induce rapid thermal desorption of the peptides (0 % to 100% in 6 s, then 100% for 4 s) caused a significant amount of in-source fragmentation because of the extra internal energy that was imparted to the ions. Compounds analyzed by LDTD usually require between 20% to 65% of maximum laser power for optimal desorption [23, 31, 46-48], however preliminary optimization tests (results not shown) demonstrated that the laser power was required to reach 100% to observe an abundant signal for the target peptides in LDTD.

This in-source fragmentation hypothesis was supported by the presence of multiple fragments that matched *b*- and *y*- ions (Figures S2-S7, Supporting information). In some cases, those fragment ions, as well $[M+H]^+$ ions, were often accompanied by their corresponding water (-18 Da) or ammonia (-17 Da) losses. Ammonia losses $[M+H-NH_3]^+$ can be observed in electrospray ionization (ESI) and are precursors of fragment b_n-NH_3 and y_n-NH_3 [49] . The formation of $[M-H_2O+H]^+$ or y_n-NH_3 ions from peptides exposed to heat has been previously reported [36, 37, 39]. However, in all those studies, heat was applied after the ionization of peptides by very soft techniques such ESI or electrosonic spray. In LDTD, the inverse process is applied: fast heating is applied first providing extra internal molecular energy and then analyte molecules are ionized by APCI. This further explains why peptide fragmentation observed in the present paper is more extensive than in previous studies [38, 40, 41].

Other peaks corresponding to *m*-ions (fragment ions arising from sidechain losses of the protonated molecule[50]) and *c*- and *x*-ions were also observed. Side-chain cleavages are observed in ionization methods that transfer high amounts of energy [49], while *c*- and *x*- ions are typically detected in electron-based activation methods, e.g., electron transfer dissociation (ETD) and high-energy activation methods such as ultraviolet photodissociation (UVPD) [51]. Therefore, in the experimental conditions used in the present study, LDTD appears to transfer a considerable amount of energy to the target peptides. This aspect will be discussed further in the following section.

While the formation of multiple fragments makes quantitative analysis of peptides by LDTD less sensitive, the fragmentation patterns observed in LDTD are complementary to those of observed in low energy collision-induced dissociation (CID) and could be applied as an alternative technique to improve amino acid sequence determination when other techniques such as ETD and UVPD may not be available. However, further experiments are necessary to confirm the reproducibility and sensitivity of LDTD for such applications.

3.3 Tandem mass spectrometry experiments

To identify the most abundant and stable fragment ions that could be used in MRM transitions for quantification purposes, it was decided to acquire product ion spectra of the most abundant ions of each peptide as well their deuterated analogues. Results of these experiments are shown on Table 1 and Figures 1-4. Those experiments allowed to confirm the composition of the precursor ions of interest for four (leu-enkephalin, endormorphin-2, IADYNYK and QIAPGQTGK) out of the six target peptides. For leu-enkephalin (Figure 1) and endomorphin-2 (Figure 2), the protonated peptide molecule was abundant enough to observe their product ions. For the rest of the target peptides, high mass fragments were selected for product ion scan experiments. In all cases, the mass spectra yielded mainly *b*-, *y*- and *a*-ions. Also, internal fragments (e.g., GF, PF, AP) and immonium ions (e.g., Y, F) were observed. NIDGYFK was the only peptide for which reproducible signals could not be obtained and further tests for this peptide were abandoned since the objective was to find optimal MRM transitions for quantification. As for GVYYPDK, full and product ion spectra of its isotopologue did not match its structure, and further experiments were abandoned as it was not possible to confirm the nature of the precursor ion (c_5 fragment) used for MRM experiments.

The product ion mass spectrum of *m/z* 556 ($[M+H]^+$) of leu-enkephalin (Figure 1), showed product ions typically observed for this peptide. However a detailed analysis of the product ions formed suggests that the precursor ion had a higher internal energy in LDTD than in previous electrospray ionization experiments [52]. The intensity ratio of a_4 and b_4 ions of leu-enkephalin was proposed by Thibault, et al. [53] as an index of the amount of internal energy deposition in the molecule. According to Vachet, et al. [54] moderately energetic CID shows an a_4/b_4 intensity ratio of 0.75. The results show that when using a collision energy of only 25 eV, it was observed that the a_4/b_4 ion ratio was 9.22, which indicates that the ions arrived at the collision cell with a high amount of internal energy resulting from the fast thermal desorption in LDTD and that the thermalization process induced by the carrier gas flow in the LDTD source [24] was not able to reduce the internal energy deposited in leu-enkephalin to thermal levels. By comparing this spectrum to one obtained by electrospray ionization in the positive mode using the same instrument and collision energy (Figure S8), it is possible to observe that in LDTD higher abundances were shifted towards product ions of lower mass-to-charge ratios due to the high energy deposition caused by the LDTD conditions employed.

Table 1. Composition of the ions of interest for quantitative analysis of the target peptides. Underlined ions indicate the product ions used form MRM transitions in the quantitative analysis.

Peptide (sequence)	**Selected ion *m/z***	**Ion type**	**Proposed composition**	**Ions identified in the product ion scan* *m/z***
Leu-enkephalin (YGGFL)	556	$[M+H]^+$	YGGFL	397 (a_4), 278 (b_3), 221 (b_2), 205 (GF), 177 (GF-CO), 136 (Y), 120 (F)
Endomorphin-2 (YPFF-NH_2)	572	$[M+H]^+$	YPFF-NH_2	<u>408 (b_3)</u>, 261 (b_2), 233 (a_2), <u>244.9 (PF)</u>, 217 (PF-CO), 136 (Y), 120 (F)
GVYYPDK	597	c_5	GVYYP	320 (b_3), 299 (YY-CO), 275 (a_3-NH_3) 157 (b_2), 136 (Y)
IADYNYK	462	c_4-H_2O	IADY	304 (ADY-CO-H_2O), 278 (NY), 261 (DY-H_2O), <u>185 (b_2)</u>, 157 (a_2), 136 (Y)
QIAPGQTGK	410	b_4	QIAP	<u>197 (a_2-NH_3)</u>, 225 (b_2-NH_3), 169 (AP)

* Product ions were confirmed with the spectral analysis of the corresponding isotopologue except for GVYYPDK.
Note: since no reproducible ion could be identified in the full scan mass spectrum of NIDGYFK, it was not included in the table.

For endomorphin-2 (Figure 2), the same observation was made, the most abundant ions in the product ion spectrum were fragments of low *m/z* : immonium ion F (*m/z* 119, relative abundance: 100 %), PF (*m/z* 245, 63.8%), b_2 (*m/z* 261, 60.4%) and a_2 (*m/z* 233, 56.0%).

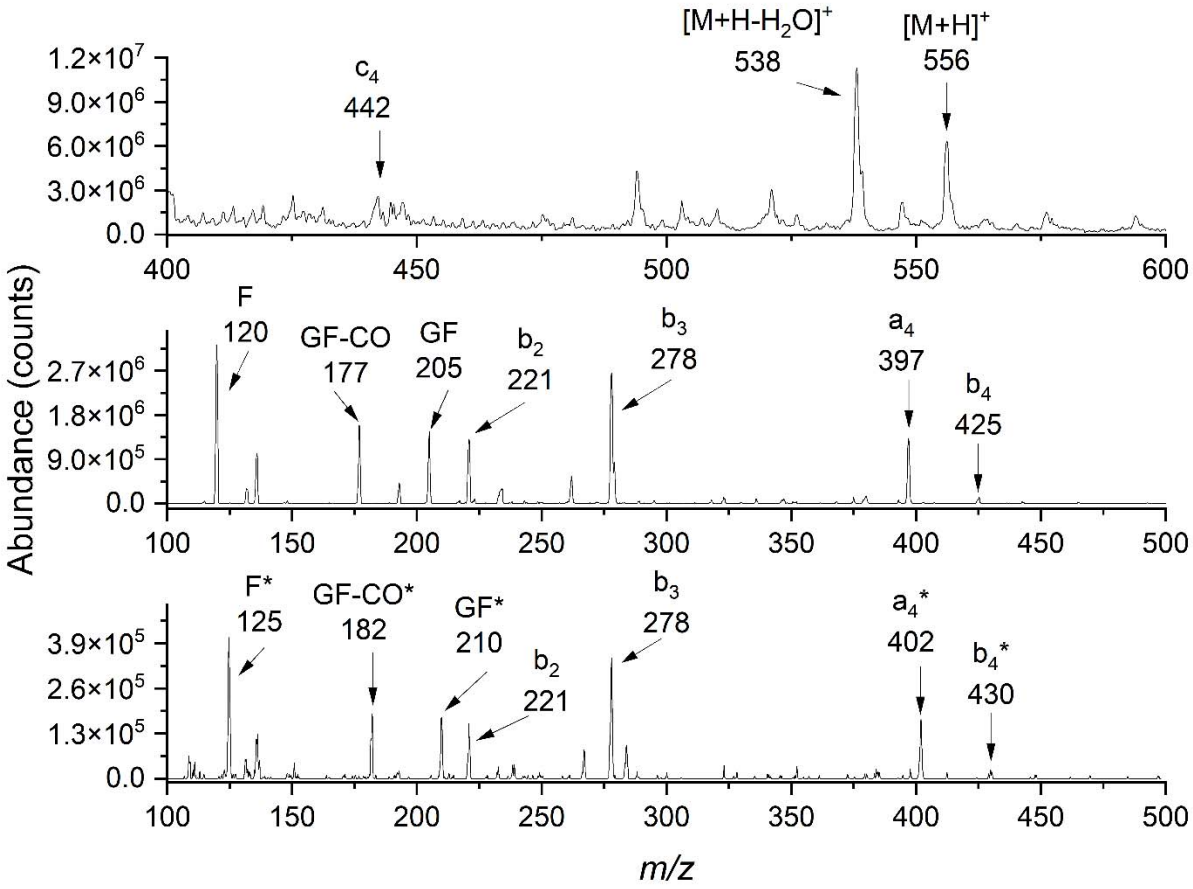

Figure 1. Full and product ion spectra of leu-enkephalin (YGGFL) obtained by LDTD in the positive mode. Top: Full-mass spectrum. Middle: Product ion mass spectrum of the $[M+H]^+$ ion (*m/z* 556) using a collision energy of 25 eV. Bottom: Product ion mass spectrum of the $[M_{d5}+H]^+$ ion (*m/z* 561) from YGGF(d_5) using a collision energy of 25 eV. The ions with an asterisk (*) indicate a mass shift due to the presence of deuterium atoms.

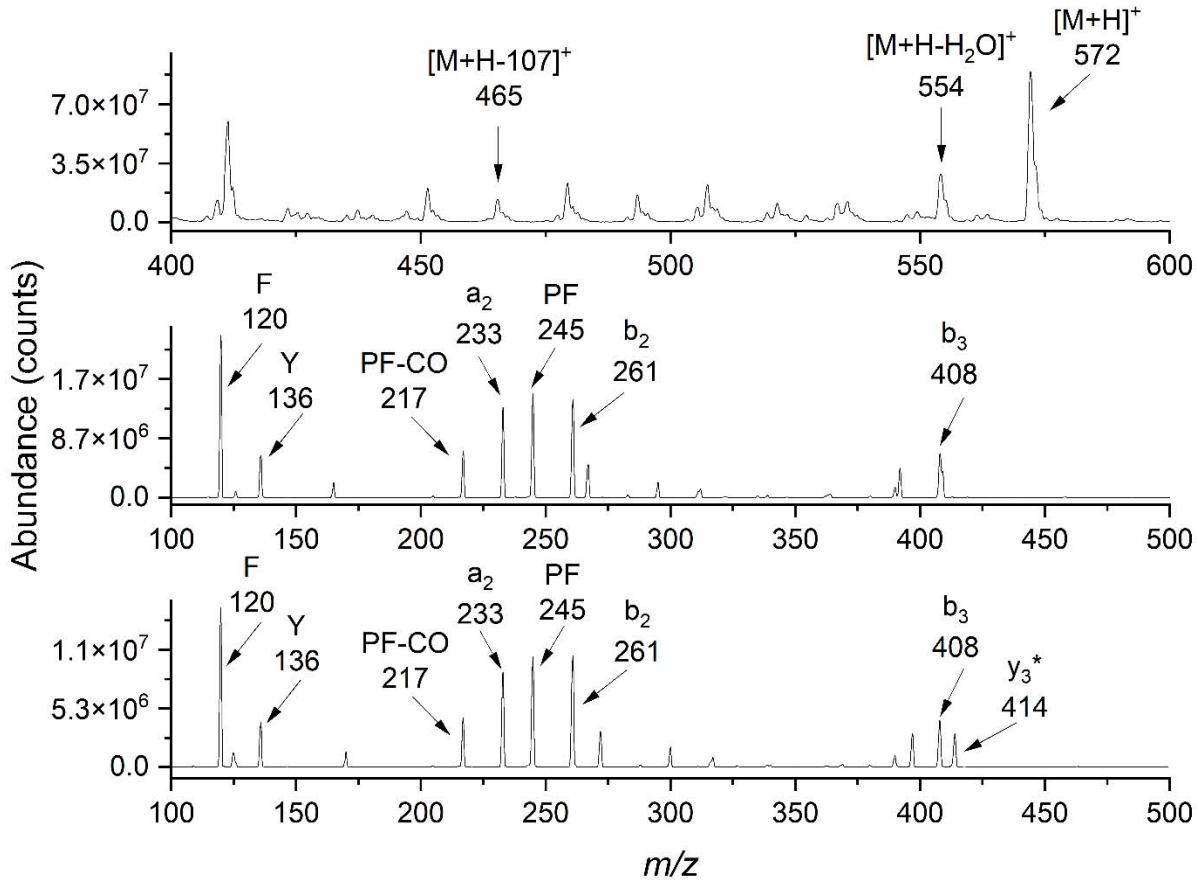

Figure 2. Full and product ion spectra of endomorphin-2 (YPFF-NH_2) obtained by LDTD in the positive mode. Top: Full-mass spectrum. Middle: Product ion mass spectrum of the $[M+H]^{+}$ ion (*m/z* 572) using a collision energy of 25 eV. Bottom: Product ion mass spectrum of the $[M_{d5}+H]^{+}$ ion (*m/z* 577) from YPFF(d_5)-NH_2. The ions with an asterisk (*) indicate a mass shift due to the presence of deuterium atoms.

For IADYNYK and QIAPGTGK, the two tryptic peptides related to the SARS-CoV-2 Spike protein, the most abundant ions (*m/z* 462 and *m/z* 410, respectively) were selected for product ion experiments (Figures 3 and 4). For both peptides, *a*- and *b*- ions were the most abundant, but in the case of QIAPGTGK only the ammonia losses were observed. The composition of the precursor ions was confirmed by performing a product ion scan experiments on the deuterated analogues.

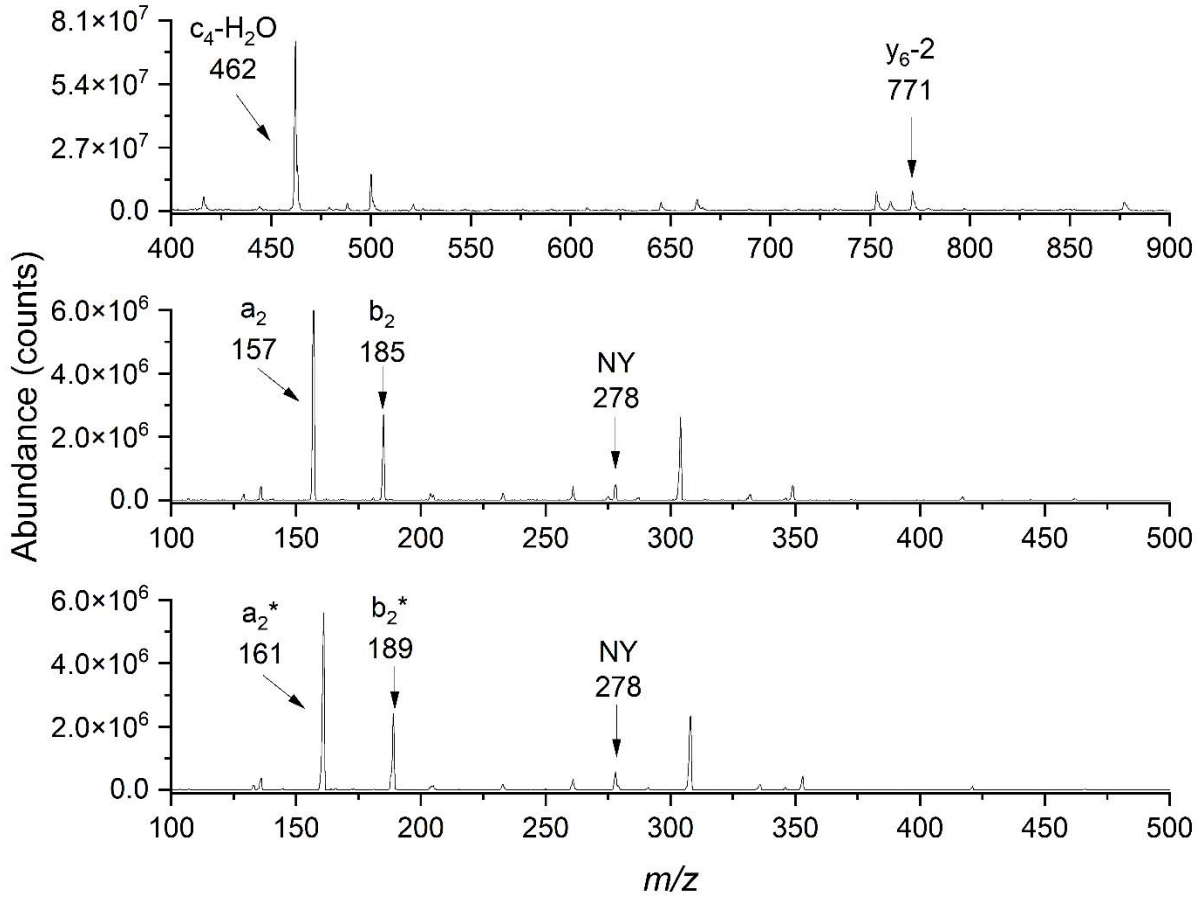

Figure 3. Full and product ion spectra of IADYNYK obtained by LDTD in the positive mode. Top: Full-mass spectrum. Middle: Product ion mass spectrum of the ion c_4-H_2O (*m/z* 462) using a collision energy of 25 eV. Bottom: Product ion mass spectrum of $c_4(d_4)$-H_2O ion (*m/z* 466) from IA(d_4)DYNYK using a collision energy of 25 eV. The ions with an asterisk (*) indicate a mass shift due to the presence of deuterium atoms.

The most abundant ion in the full mass spectrum of IA(d_4)DYNYK was *m/z* 466 (results not shown) and product ion experiments showed the presence of *m/z* 161 and *m/z* 189 corresponding to $a_2(d_4)$ and $b_2(d_4)$, respectively in its spectrum (Figure 3). Therefore, the composition of *m/z* 462, the precursor ion of IADYNYK selected for MRM experiments, corresponds well to a c_4-H_2O ion of amino acid composition IADY. In the case of QIA(d_4)PGTGK, no mass shift was observed for the ions corresponding to a_2-NH_3 (*m/z* 197) and b_2-NH_3 (*m/z* 225) since the deuterated alanine moiety was absent in the amino acid composition (QI). However the internal A(d_4)P ion was observed which confirmed that the composition of *m/z* 410, the precursor ion of QIAPGTGK selected for MRM experiments corresponds well to a b_4 ion of amino acid composition QIAP.

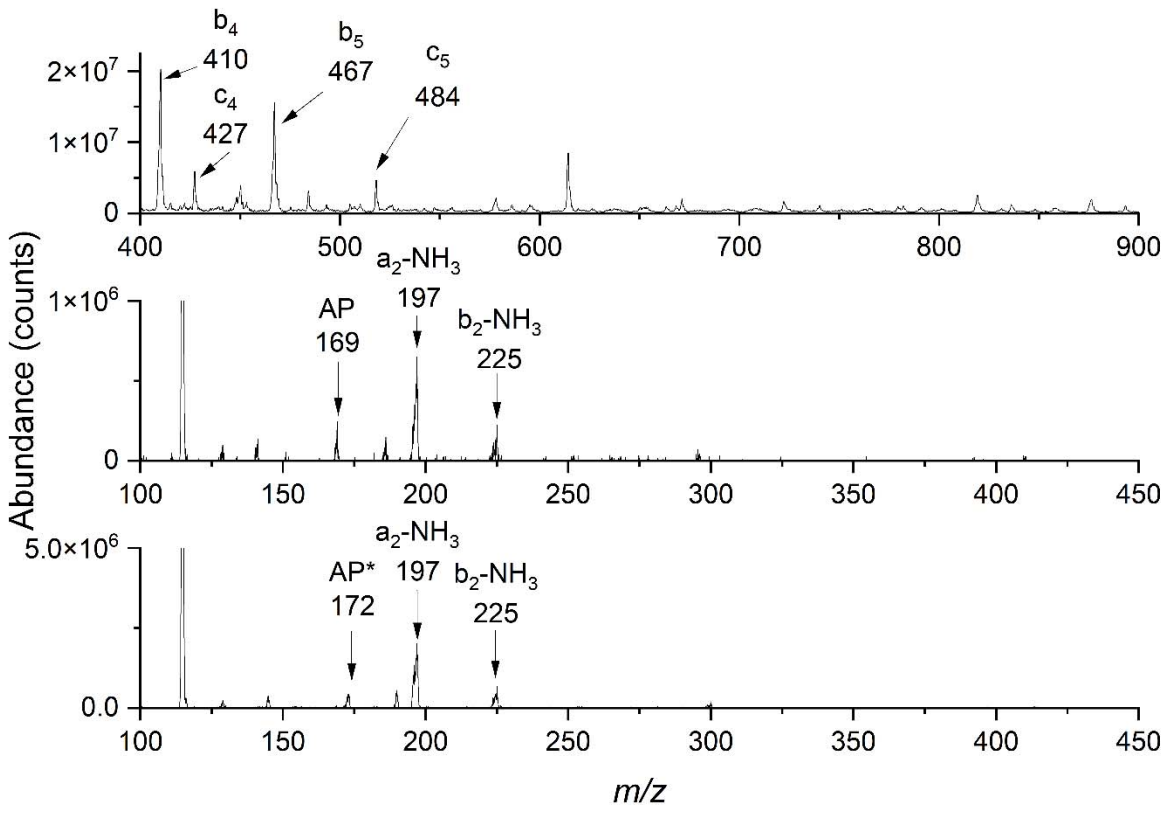

Figure 4. Full and product ion spectra of QIAPGTGK obtained by LDTD in the positive mode. Top: Full-mass spectrum. Middle: Product ion mass spectrum of the ion b_4 (*m/z* 410) using a collision energy of 25 eV. Bottom: Product ion mass spectrum of the b_4 ion (*m/z* 410) from QIA(d_4)PGQTGK using a collision energy of 25 eV. The ions with an asterisk (*) indicate a mass shift due to the presence of deuterium atoms.

3.4 Quantification

Three peptides were selected for quantitative analysis: endormorphin-2, as a model for small (< 600 Da) peptides as well as IADYNYK and QIAPGTGK, since they are two tryptic peptides related to the Spike protein of SARS-CoV-2. These peptides were quantified by internal calibration using their corresponding deuterated analogues in two different conditions: a solvent mixture and spiked in 20 µg mL^{-1} of digested bovine serum albumin (BSA).

Results of the quantification of endomorphin-2 in both the solvent mixture and in the presence of digested BSA (Table 2) showed that calibration curves were linear ($R^2 > 0.99$) and trueness and precision were better than accepted quality assurance criteria (bias : -20% to +10%, relative standard deviation: between 11.3% and 16%) [55]. However, it was observed that the dynamic range was narrow, concentrations spanning less than 2 orders of magnitude could be quantified, and

LOQ were in the 0.5-2 μg mL^{-1} range, which is relatively high for a tandem mass spectrometry technique. When testing the MRM transitions for quantitative analysis, it was observed that the *m/z* 572 → *m/z* 408 transition, used for analysis in the solvent mixture, was less effective in the presence of BSA tryptic peptides, probably due to the presence of interferences. Therefore, the MRM transition *m/z* 572 → *m/z* 245 was used for the quantification of endomorphin-2 instead. Interestingly, the LOQ were better in the samples spiked with digested BSA, which may be due to the "coating effect" of a matrix in LDTD. It has been shown that coating the surface of LDTD microwell plates with small organic acids [56] or proteins [46] enhanced the signal for multiple small molecules. Such effect was explained by changes in the crystallization of the analytes deposited in the microwells. Indeed, smaller crystals and higher amounts of amorphous phase favour the fast thermal desorption of analytes and thus increase their signals in LDTD. It is not clear if the presence of tryptic BSA peptides in the samples also could decrease the thermal degradation of endomorphin-2, and additional experiments are necessary to understand the "coating effect" in LDTD when using the maximum laser power output.

For IADYNYK and QIAPGQTGK, results (Table 2) also showed that the analysis in the solvent mixture had a worse performance than in the presence of digested BSA. For IADYNYK, the relative standard deviation improved of almost 10 percentage units, and for QIAPGQTGK bias improved nearly 25 percentage units in the samples spiked with the BSA digest. Such result is well explained by the "coating effect" mentioned previously which also better the LOQ.

A substantial difference was observed between LOD and LOQ values (Table 2) which is due to the definitions used. For the LOD, the standard deviation of 10 matrix blank samples times a *k* factor of 3 divided by the calibration curve slope was employed. For the LOQ, the concentration of the lowest standard with a bias percentage ≤ ±20 % was used. Therefore, the LOD only considers if the analyte signal is higher than the background and does not take into account trueness, which at low concentrations (0.01 μg mL^{-1}) reached 10000% bias for AIDYNYK.

Overall, the selectivity of the method is also well demonstrated by the MRM ion current desorption profiles shown in Figure 5. As it can be seen, peaks at the LOQ of each peptide were significantly higher than the noise from the matrix. However, quantitative analysis remains limited because of the narrow dynamic range and the relatively high LOQ (endomorphhin-2: 0.5 μg mL^{-1}, IADYNYK: 1 μg mL^{-1}, QIAPGQTGK: 1.5 μg mL^{-1}). Appropriate LOD and LOQ levels depend on the intended application. In the case of clinical applications for detection of viruses such as SARS-CoV-2, based on reported median viral loads in patients obtained using Real-Time Quantitative Reverse Transcription (RT-PCR) of throat swabs[57], it is estimated that LOQ for characteristic peptides such as IADYNYK and QIAPGQTGK should be ≈3.5 fg mL^{-1}, i.e. ≈10^8 times lower than the experimental LOQ reported here. RT-PCR methods are the gold standard for viral analysis of clinical samples and they are able to detect as few as 1000 RNA copies per milliliter [58]. For other applications, such as the detection of protein allergens in food, detection levels as low as 1 mg of protein are desirable [59]. For example, in the case of caseins in milk LOQ for peptides ≈500-900 Da should be ≈21-47 μg mL^{-1} which are of the same order of magnitude as the values reported here. For a detailed calculation on how the expected LOQ values were obtained, please consult the Supporting Information.

In summary, assays showed that quantitative analysis of endomorphin-2, IADTNYK and QIAPGQTGK in a protein digest was possible by LDTD and the main figures of merit (calibration

curve linearity, precision, and trueness) were acceptable, but LOD/LOQ values remain too high for applications where trace amounts of proteins (< 0.1 μg mL^{-1}) need to be quantified. However other applications where higher levels of proteins must be detected, such as quality control or detection of protein allergens, could be possible by LDTD.

Table 2. Quantification data of endomorphin-2, IADYNYK and QIAPGQTGK in the solvent, and parameters for tandem mass analysis using MRM acquisition mode.

	Solvent mixture		BSA spiked (20 µg mL^{-1})								
Compounds / MRM transtition	**R²**	**LOQ (µg mL^{-1})**	**Dynamic range (µg mL^{-1})**	**Trueness* (bias %)**	**Precision* (RSD %)**	**R²**	**LOD (µg mL^{-1})**	**LOQ (µg mL^{-1})**	**Dynamic range (µg mL^{-1})**	**Trueness* (bias %)**	**Precision* (RSD %)**
Endomorphin-2 *m/z* 572 → *m/z* 408† *m/z* 572 → *m/z* 245‡	0.9976	2	2-20	-3.8 [a]	1.6 [a]	0.9980	0.0004	0.5	0.5-15	-0.03 [b]	4.9 [b]
IADYNYK *m/z* 462 → *m/z* 185	0.9815	5	5-40	-19.7 [c]	6.9 [c]	0.9791	0.02	1.5	1.5-20	8.3 [d]	18.2 [d]
QIAPGQTGK *m/z* 410→ *m/z* 197	0.9725	10	10-40	25.2 [d]	3.0 [d]	0.9910	0.1	1	1-30	0.87 [c]	11.4 [c]

***** Trueness and precision were evaluated at: [a] 8 µg mL^{-1}; [b] 2 µg mL^{-1}; [c] 6 µg mL^{-1} ; [d] 15 µg mL^{-1}. † MRM transition used for quantification in the solvent. ‡ MRM transition used for quantification in the BSA matrix.

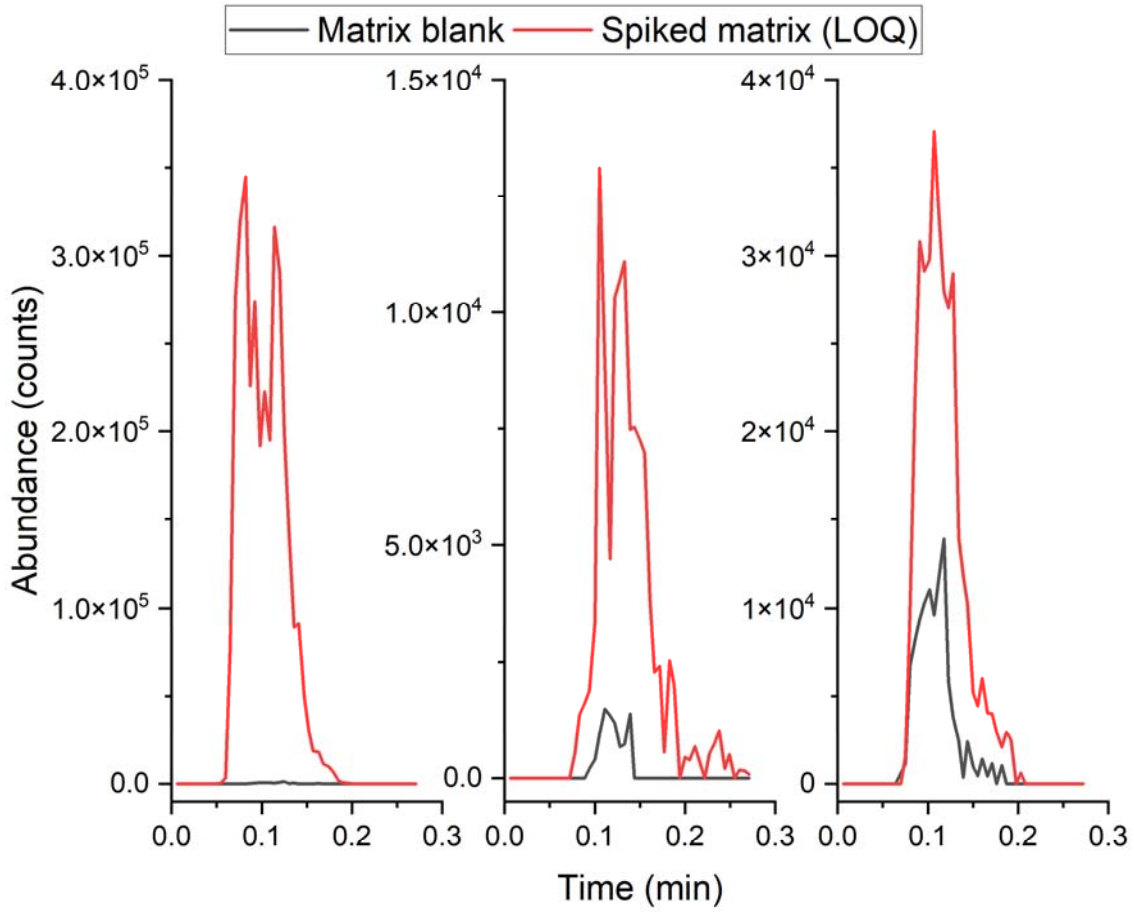

Figure 5. MRM ion current desorption profiles of the quantified peptides spiked at their LOQ levels in digested BSA matrix. Left: endomorphin-2 (*m/z* 572 → *m/z* 245, LOQ: 0.5 µg mL^{-1}), center: IADYNYK (*m/z* 462 → *m/z* 185, LOQ: 1.5 µg mL^{-1}) and right: QIAPGQTGK (*m/z* 410→ *m/z* 197, LOQ: 1 µg mL^{-1}).

4. Conclusion

The present study demonstrated for the first time that it is possible to analyze qualitatively and quantitatively peptides by LDTD-QqQMS. Upon rapid thermal desorption, the target peptides were fragmented, many abundant product ions were identified and corresponded to *b*-, *y*-, *c*- or *x*-ions and related H_2O or NH_3 losses. While such fragmentation does impact quantitative applications, LDTD offers alternative structural information that cannot be obtained by collision-induced dissociation. Trueness and precision for the quantification of endomorphin-2, IADTNYK and QIAPGQTGK was equal or better than acceptable criteria. However, both LOQ and dynamic range remained inadequate for trace analysis applications. Future studies should find new approaches to improve those two figures of merit.

Many questions still remain regarding the desorption and ionization of peptides by LDTD. Multiple in peaks in the mass spectrum were unidentified and it was not clear why some peptides had higher and more stable signals than others. Given the advantages of LDTD for high-throughput applications (> 15 000 samples in a single sequence and in less than 43 h), such questions should be answered in order to develop fully functional quantitative analysis methods for peptides by LDTD-QqQMS.

Acknowledgments

We thank Serge Auger and Pierre Picard from Phytronix for fruitful discussions about the LDTD source. This project was funded by the National Sciences and Engineering Research Council of Canada (NSERC Alliance COVID-19, Grant Number: ALLRP 554601-20). Laboratory equipment was funded by the National Sciences and Engineering Research Council of Canada (RTI Grant), the Canadian Foundation for Innovation (CFI) and the Fonds de Recherche du Québec (FRQ), and the Government of Quebec (CFI John R. Evans Leaders Grant). F. Beaudry is the holder of the Canada Research Chair in metrology of bioactive molecules and target discovery (Grant number: CRC-2021-00160).

CRediT author statement

Pedro A. Segura: Conceptualization, Methodology, Validation, Formal analysis, Investigation, Writing – Original Draft, Writing – Review & Editing, Visualization, Supervision, Project administration, Funding acquisition
Cédric Guillaumain: Formal analysis, Investigation, Validation, Writing – Original Draft, Visualization
Emmanuel Eysseric: Investigation, Supervision
Judith Boudrias: Validation, Investigation
Mégane Moreau : Investigation
Cassandra Guérette: Investigation
Rémi Clemencin: Investigation
Francis Beaudry: Resources, Writing – Original Draft, Writing, Writing – Review & Editing, Supervision, Funding acquisition

5. References

[1] F. Wu, S. Zhao, B. Yu, Y.-M. Chen, W. Wang, Z.-G. Song, Y. Hu, Z.-W. Tao, J.-H. Tian, Y.-Y. Pei. A new coronavirus associated with human respiratory disease in China. *Nature* **2020**, *579*, 265.

[2] G. Guglielmi. Fast coronavirus tests: what they can and can't do. *Nature* **2020**, *585*, 496.

[3] G. Guglielmi. Rapid coronavirus tests: a guide for the perplexed. *Nature* **2021**, *590*, 202.

[4] P. K. Drain. Rapid diagnostic testing for SARS-CoV-2. *New England journal of medicine* **2022**, *386*, 264.

[5] J. Lan, J. Ge, J. Yu, S. Shan, H. Zhou, S. Fan, Q. Zhang, X. Shi, Q. Wang, L. Zhang. Structure of the SARS-CoV-2 spike receptor-binding domain bound to the ACE2 receptor. *Nature* **2020**, *581*, 215.

[6] R. Yan, Y. Zhang, Y. Li, L. Xia, Y. Guo, Q. Zhou. Structural basis for the recognition of SARS-CoV-2 by full-length human ACE2. *Science* **2020**, *367*, 1444.

[7] D. Martínez-Flores, J. Zepeda-Cervantes, A. Cruz-Reséndiz, S. Aguirre-Sampieri, A. Sampieri, L. Vaca. SARS-CoV-2 vaccines based on the spike glycoprotein and implications of new viral variants. *Frontiers in immunology* **2021**, *12*.

[8] Y.-C. Hwang, R.-M. Lu, S.-C. Su, P.-Y. Chiang, S.-H. Ko, F.-Y. Ke, K.-H. Liang, T.-Y. Hsieh, H.-C. Wu. Monoclonal antibodies for COVID-19 therapy and SARS-CoV-2 detection. *Journal of Biomedical Science* **2022**, *29*, 1.

[9] T. Perkmann, N. Perkmann-Nagele, T. Koller, P. Mucher, A. Radakovics, R. Marculescu, M. Wolzt, O. F. Wagner, C. J. Binder, H. Haslacher. Anti-spike protein assays to determine SARS-CoV-2 antibody levels: a head-to-head comparison of five quantitative assays. *Microbiology spectrum* **2021**, *9*, e00247.

[10] BBC News. Covid PCR tests end for asymptomatic cases in England. BBC News Services, 2022**.** https://www.bbc.com/news/uk-59944057. Accessed 2022-02-10.

[11] CBC News. Quebec stops PCR tests for general public as Omicron overwhelms system. CBC/Radio-Canada, 2022**.** https://www.cbc.ca/news/canada/montreal/pcr-tests-stopped-omicron-quebec-1.6304313. Accessed 2022-02-10.

[12] C. J. Welch. High throughput analysis enables high throughput experimentation in pharmaceutical process research. *Reaction Chemistry & Engineering* **2019**, *4*, 1895.

[13] WHO. Antigen-detection in the diagnosis of SARS-CoV-2 infection. 2021**.** https://www.who.int/publications/i/item/antigen-detection-in-the-diagnosis-of-sars-cov-2infection-using-rapid-immunoassays. Accessed 2022-06-30.

[14] R. Aebersold, M. Mann. Mass spectrometry-based proteomics. *Nature* **2003**, *422*, 198.

[15] R. Aebersold, M. Mann. Mass-spectrometric exploration of proteome structure and function. *Nature* **2016**, *537*, 347.

[16] F. Meissner, J. Geddes-McAlister, M. Mann, M. Bantscheff. The emerging role of mass spectrometry-based proteomics in drug discovery. *Nature Reviews Drug Discovery* **2022**, 1.

[17] M. van Bentum, M. Selbach. An introduction to advanced targeted acquisition methods. *Molecular & Cellular Proteomics* **2021**, *20*.

[18] P. Picotti, R. Aebersold. Selected reaction monitoring–based proteomics: workflows, potential, pitfalls and future directions. *Nature methods* **2012**, *9*, 555.

[19] A. Doerr. Mass spectrometry–based targeted proteomics. *Nature methods* **2013**, *10*, 23.

[20] M. J. Wither, K. C. Hansen, J. A. Reisz. Mass spectrometry-based bottom-up proteomics: Sample preparation, LC-MS/MS analysis, and database query strategies. *Current Protocols in Protein Science* **2016**, *86*, 16.4. 1.

[21] S. Pan, R. Aebersold, R. Chen, J. Rush, D. R. Goodlett, M. W. McIntosh, J. Zhang, T. A. Brentnall. Mass spectrometry based targeted protein quantification: methods and applications. *Journal of proteome research* **2009**, *8*, 787.

[22] D. C. Liebler, L. J. Zimmerman. Targeted quantitation of proteins by mass spectrometry. *Biochemistry* **2013**, *52*, 3797.

[23] P. B. Fayad, M. Prévost, S. Sauvé. Laser Diode Thermal Desorption-Atmospheric Pressure Chemical Ionization Tandem Mass Spectrometry Analysis of Selected Steroid Hormones in Wastewater: Method Optimization and Application. *Analytical Chemistry* **2010**, *82*, 639.

[24] P. A. Segura, P. Tremblay, P. Picard, C. Gagnon, S. Sauvé. High-Throughput Quantitation of Seven Sulfonamide Residues in Dairy Milk using Laser Diode Thermal Desorption-Negative Mode Atmospheric Pressure Chemical Ionization Tandem Mass Spectrometry. *Journal of Agricultural and Food Chemistry* **2010**, *58*, 1442.

[25] J. J. Lohne, W. C. Andersen, S. B. Clark, S. B. Turnipseed, M. R. Madson. Laser diode thermal desorption mass spectrometry for the analysis of quinolone antibiotic residues in aquacultured seafood. *Rapid Communications in Mass Spectrometry* **2012**, *26*, 2854.

[26] G. Blachon, P. Picard, P. Tremblay, S. Demers, R. Paquin, P. B. Fayad. Rapid Determination of Chloramphenicol in Honey by Laser Diode Thermal Desorption Using Atmospheric Pressure Chemical Ionization-Tandem Mass Spectrometry. *Journal of AOAC International* **2013**, *96*, 676.

[27] J.-F. Jourdil, P. Picard, C. Meunier, S. Auger, F. Stanke-Labesque. Ultra-fast cyclosporin A quantitation in whole blood by Laser Diode Thermal Desorption–Tandem Mass Spectrometry; comparison with High Performance Liquid Chromatography–Tandem Mass Spectrometry. *Analytica chimica acta* **2013**, *805*, 80.

[28] O. Heudi, S. Barteau, P. Picard, P. Tremblay, F. Picard, O. Kretz. Laser diode thermal desorption–positive mode atmospheric pressure chemical ionization tandem mass spectrometry for the ultra-fast quantification of a pharmaceutical compound in human plasma. *Journal of pharmaceutical and biomedical analysis* **2011**, *54*, 1088.

[29] J. G. Swales, R. T. Gallagher, M. Denn, R. M. Peter. Simultaneous quantitation of metformin and sitagliptin from mouse and human dried blood spots using laser diode thermal desorption tandem mass spectrometry. *Journal of pharmaceutical and biomedical analysis* **2011**, *55*, 544.

[30] J. G. Swales, D. G. Temesi, M. Denn, K. Murphy. Determination of paracetamol in mouse, rat and dog plasma samples by laser diode thermal desorption–APCI-MS/MS. *Bioanalysis* **2012**, *4*, 1327.

[31] A. Borik, A. V. Stanova, R. Kodesova, B. Brooks, K. Grabicova, P. Novakova, R. Grabic. Ultrafast laser diode thermal desorption method for analysis of representative pharmaceuticals in soil leachate samples. *Talanta* **2020**, *208*, 120382.

[32] M. Boisvert, P. B. Fayad, S. Sauve. Development of a new multi-residue laser diode thermal desorption atmospheric pressure chemical ionization tandem mass spectrometry method for the detection and quantification of pesticides and pharmaceuticals in wastewater samples. *Analytica Chimica Acta* **2012**, *754*, 75.

[33] M. Solliec, D. Massé, S. Sauvé. Analysis of trimethoprim, lincomycin, sulfadoxin and tylosin in swine manure using laser diode thermal desorption-atmospheric pressure chemical ionization-tandem mass spectrometry. *Talanta* **2014**, *128*, 23.
[34] J. J. Coon, W. Harrison. Laser desorption-atmospheric pressure chemical ionization mass spectrometry for the analysis of peptides from aqueous solutions. *Analytical chemistry* **2002**, *74*, 5600.
[35] S. Cristoni, L. R. Bernardi, I. Biunno, F. Guidugli. Analysis of peptides using partial (no discharge) atmospheric pressure chemical ionization conditions with ion trap mass spectrometry. *Rapid communications in mass spectrometry* **2002**, *16*, 1686.
[36] M. Meot-Ner, A. R. Dongré, A. Somogyi, V. H. Wysocki. Thermal decomposition kinetics of protonated peptides and peptide dimers, and comparison with surface-induced dissociation. *Rapid communications in mass spectrometry* **1995**, *9*, 829.
[37] H. Chen, L. S. Eberlin, R. G. Cooks. Neutral fragment mass spectra via ambient thermal dissociation of peptide and protein ions. *Journal of the American Chemical Society* **2007**, *129*, 5880.
[38] S. Zhang, F. Basile. Site-specific pyrolysis-induced cleavage at aspartic acid residue in peptides and proteins. *Journal of proteome research* **2007**, *6*, 1700.
[39] M. A. Meetani, O. K. Zahid, J. Michael Conlon. Investigation of the pyrolysis products of methionine-enkephalin-Arg-Gly-Leu using liquid chromatography–tandem mass spectrometry. *Journal of mass spectrometry* **2010**, *45*, 1320.
[40] F. Basile, S. Zhang, S. K. Kandar, L. Lu. Mass spectrometry characterization of the thermal decomposition/digestion (TDD) at cysteine in peptides and proteins in the condensed phase. *Journal of the American Society for mass Spectrometry* **2011**, *22*.
[41] M. O. Altmeyer, A. Manz, P. Neužil. Microfluidic Superheating for Peptide Sequence Elucidation. *Analytical Chemistry* **2015**, *87*, 5997.
[42] B. Orsburn, C. Jenkins, S. M. Miller, B. A. Neely, N. M. Bumpus. In silico approach toward the identification of unique peptides from viral protein infection: Application to COVID-19. *BioRxiv* **2020**.
[43] G. L. Long, J. D. Winefordner. Limit of Detection: A Closer Look at the IUPAC Definition. *Analytical Chemistry* **1983**, *55*, 712A.
[44] W. C. Andersen, M. VanSickle, J. Storey, V. Sheldon, J. Lohne, S. B. Turnipseed, T. Thomas, M. Madson. Fast analysis of caffeinated beverages using laser diode thermal desorption mass spectrometry (LDTD-MS/MS). *Food Additives & Contaminants: Part A* **2019**, *36*, 1616.
[45] E. Jagerdeo, S. Auger. Rapid screening procedures for a variety of complex forensic samples using laser diode thermal desorption (LDTD) coupled to different mass spectrometers. *Rapid Communications in Mass Spectrometry* **2022**, *36*, e9244.
[46] A. Gravel, C. Guérette, D. Fortin, S. Auger, P. Picard, P. A. Segura. Further studies on the signal enhancement effect in laser diode thermal desorption-triple quadrupole mass spectrometry using microwell surface coatings. *Journal of Mass Spectrometry* **2019**, *54*, 948.
[47] L. Lonappan, R. Pulicharla, T. Rouissi, S. K. Brar, M. Verma, R. Y. Surampalli, J. R. Valero. Diclofenac in municipal wastewater treatment plant: quantification using laser diode thermal desorption—atmospheric pressure chemical ionization—tandem mass spectrometry approach in comparison with an established liquid chromatography-

electrospray ionization–tandem mass spectrometry method. *Journal of Chromatography A* **2016**, *1433*, 106.
[48] A. Roy-Lachapelle, P. B. Fayad, M. Sinotte, C. Deblois, S. Sauvé. Total microcystins analysis in water using laser diode thermal desorption-atmospheric pressure chemical ionization-tandem mass spectrometry. *Analytica chimica acta* **2014**, *820*, 76.
[49] V. H. Wysocki, K. A. Resing, Q. Zhang, G. Cheng. Mass spectrometry of peptides and proteins. *Methods* **2005**, *35*, 211.
[50] K. F. Medzihradszky, A. L. Burlingame. The advantages and versatility of a high-energy collision-induced dissociation-based strategy for the sequence and structural determination of proteins. *Methods* **1994**, *6*, 284.
[51] J. S. Brodbelt. Ion activation methods for peptides and proteins. *Analytical chemistry* **2016**, *88*, 30.
[52] J. Sztáray, A. Memboeuf, L. Drahos, K. Vékey. Leucine enkephalin—a mass spectrometry standard. *Mass spectrometry reviews* **2011**, *30*, 298.
[53] P. Thibault, A. Alexander, R. Boyd, K. Tomer. Delayed dissociation spectra of survivor ions from high-energy collisional activation. *Journal of the American Society for Mass Spectrometry* **1993**, *4*, 845.
[54] R. W. Vachet, K. L. Ray, G. L. Glish. Origin of product ions in the MS/MS spectra of peptides in a quadrupole ion trap. *Journal of the American Society for Mass Spectrometry* **1998**, *9*, 341.
[55] I. Taverniers, M. De Loose, E. Van Bockstaele. Trends in quality in the analytical laboratory. II. Analytical method validation and quality assurance. *TrAC Trends in Analytical Chemistry* **2004**, *23*, 535.
[56] A. Dion-Fortier, A. Gravel, C. Guérette, F. Chevillot, S. Blais, S. Auger, P. Picard, P. A. Segura. Signal enhancement in laser diode thermal desorption-triple quadrupole mass spectrometry analysis using microwell surface coatings. *Journal of Mass Spectrometry* **2019**, *54*, 167.
[57] Y. Pan, D. Zhang, P. Yang, L. L. Poon, Q. Wang. Viral load of SARS-CoV-2 in clinical samples. *The Lancet infectious diseases* **2020**, *20*, 411.
[58] M. N. Esbin, O. N. Whitney, S. Chong, A. Maurer, X. Darzacq, R. Tjian. Overcoming the bottleneck to widespread testing: a rapid review of nucleic acid testing approaches for COVID-19 detection. *RNA* **2020**, *26*, 771.
[59] D. A. Moneret-Vautrin, G. Kanny. Update on threshold doses of food allergens: implications for patients and the food industry. *Current Opinion in Allergy and Clinical Immunology* **2004**, *4*, 215.